Photochemistry and Photobiology, 2003, 77(2): 121–128

Photochemistry and Photophysics of Thienocarbazoles¶

J. Seixas de Melo*[1], L. M. Rodrigues[1], C. Serpa[1], L. G. Arnaut[1], I. C. F. R. Ferreira[2] and M.-J. R. P. Queiroz[2]

[1]Department of Chemistry (CQC), University of Coimbra, Coimbra, Portugal and
[2]Department of Chemistry, University of Minho, Braga, Portugal

Received 2 July 2002; accepted 11 November 2002

ABSTRACT

Two methylated thienocarbazoles and two of their synthetic nitro-precursors have been examined by absorption, luminescence, laser flash photolysis and photoacoustic techniques. Their spectroscopic and photophysical characterization involves fluorescence spectra, fluorescence quantum yields and lifetimes, and phosphorescence spectra and phosphorescence lifetimes for all the compounds. Triplet–singlet difference absorption spectra, triplet molar absorption coefficients, triplet lifetimes, intersystem crossing $S_1 \sim\sim\rightarrow T_1$ and singlet molecular oxygen yields were obtained for the thienocarbazoles. In the case of the thienocarbazoles it was found that the lowest-lying singlet and triplet excited states, S_1 and T_1, are of π,π^* origin, whereas for their precursors S_1 is n,π^*, and T_1 is π,π^*. In both thienocarbazoles it appears that the thianaphthene ring dictates the $S_1 \sim\sim\rightarrow T_1$ yield, albeit there is less predominance of that ring in the triplet state of the linear thienocarbazole, which leads to a decrease in the observed ϕ_T value.

INTRODUCTION

The search for new compounds with potential photosensitization activity for biological systems is relevant to the science of photobiology. An enormous number of naturally occurring and synthetic compounds are known to be photosensitizers commonly used in photobiological studies (1). In the broad field of photobiology there is particular interest in photodynamic therapy (PDT), where the search for new compounds is currently an intense field of research.

Classical examples of sensitizers used are porphyrin derivatives, particularly those based on hematoporphyrin, of which Photofrin® (commercial preparation of hematoporphyrin derivative) is the most widely used compound in PDT treatment (2). Phthalocyanines (3), halogenated porphyrins (4), chlorines (5), *etc*. all belong to the so-called new generation of photosensitizers, but all have cyclic tetrapyrrole structures closely related to hematoporphyrin. There is interest in the use of different families of compounds in this area, and the thienocarbazoles reported here are considered to be new ring D bioisosteres of pyridocarbazoles, ellipticines and olivalicines, which have known antitumor activity (6). The potential use of these as markers or in phototherapy applications has been proposed (7). The importance for biological activity of the methylated derivatives of these compounds has been stressed elsewhere (8,9).

Classical issues in the search for new photosensitizers (in particular, PDT drugs) are relatively low toxicity, selective retention in malignant tissues and absorption in the long-wavelength end of the red spectral region, where light penetration of tissue is better. Other important factors to be considered include location of malignant cells using fluorescence emission of probes and good triplet and sensitized singlet oxygen yields (2).

The following photocharacterization must be accomplished to demonstrate the potential of any particular sensitizer for photosensitization activity: (1) absorption spectrum; (2) fluorescence spectrum, quantum yield and lifetime; (3) quantitative quantum yield of triplet occupation (ϕ_T) and triplet–triplet absorption spectrum; (4) triplet state decay times (both low-temperature phosphorescence [τ_{Ph}] and room temperature [RT] triplet state lifetime [τ_T]); (5) singlet oxygen ($^1O_2$) quantum yield (ϕ_Δ); (6) triplet state energies; and (7) determination of transients that may result from electron donation or acceptance, or H atom donation or acceptance.

Although all the above aspects are obviously very important, some of these, particularly 2, 3, 4, 5, and 7, may be dependent on the environment (solvent, pH, *etc*.) (10). In this work particular emphasis will be placed on points 1–6 for the compounds studied here.

The thienocarbazoles can be considered as resulting from the linking of a carbazole (CBZ) unit to a thiophene. They also can be considered as possessing carbazole and benzothiophene (thianaphthene [TN]) units with a common benzene ring. For this purpose two parent compounds also were investigated. In Scheme 1 we present the structures of the compounds studied and the abbreviated designations used here. The synthesis and detailed characterization of the compounds studied can be found in Ferreira *et al*. (9). The main difference between the two methylated

---

¶Posted on the website on 25 November 2002.

*To whom correspondence should be addressed at: Department of Chemistry (CQC), University of Coimbra, 3004-535 Coimbra, Portugal. Fax: 351-239-827703; e-mail: sseixas@ci.uc.pt

Abbreviations: AM1-CI, Austin Model 1 with configuration interaction; BrDMA, *N,N*-bromodimethylaniline; CBZ, carbazole; HOMO, highest occupied molecular orbital; CI, configuration interaction; ISC, intersystem crossing; LT, low temperature; LUMO, lowest unoccupied molecular orbital; 2mPTC, dimethyl thienocarbazole precursor; 3mPTC, trimethyl thienocarbazole precursor; OP, optical density; PAC, photoacoustic calorimetry; PDT, photodynamic therapy; RT, room temperature; TCA, angular thienocarbazole; TCL, linear thienocarbazole; TCSPC, time-correlated single-photon counting; TN, thianaphthene; ZINDO-CI/S, Zerner intermediate neglect of differential overlap/spectroscopy with configuration interaction.

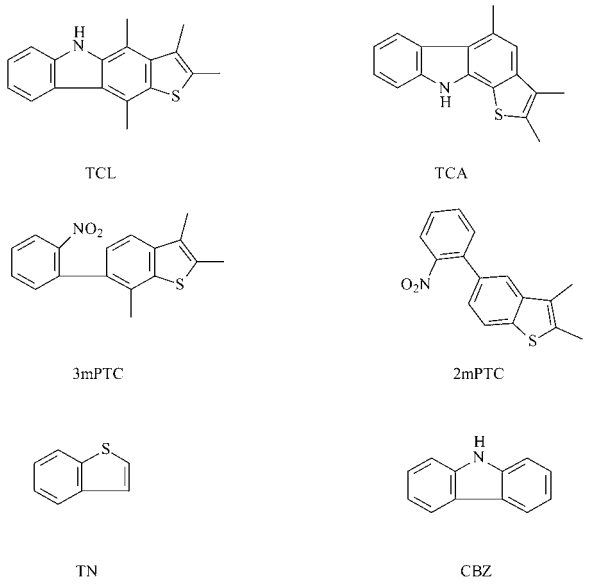

Scheme 1.

thienocarbazoles is in the position of the thiophene ring relative to the CBZ unit. In one case (linear thienocarbazole [TCL]) the two ring systems are colinear, whereas in the other system (angular thienocarbazole [TCA]) the thiophene ring is at an angle relative to the CBZ ring. For the precursors the differences are in the number of methyl substituents, two for dimethyl thienocarbazole precursor (2mPTC) and three for trimethyl thienocarbazole precursor (3mPTC), and in the position of the C–C diaryl bond in the benzo[*b*]thiophene moiety. It is advisable to state that if we strictly consider the thienocarbazole structures studied here, we are not comparing them with their exact synthetic precursors. This is so because the methyl groups are not exactly in their original positions.

Alternative ways of interaction with cell targets may not involve photodynamic mechanisms of Type I or II. It is likely that the thienocarbazole's way of action involves photocycloaddition to DNA bases, preventing its subsequent replication (9). Antioxidative properties also have been reported for other thienocarbazole derivatives, which implicitly expands the field of action of these compounds to protection against oxidative stress (11).

To our knowledge this is the first time that a complete photophysical study has been undertaken on these compounds (or similar thienocarbazoles). Work in progress involves the photophysical characterization of other substituted thienocarbazoles and their corresponding diarylamine benzo[b]thiophene precursors (7). The potential ways of action of these compounds also should be considered, namely, the evaluation of their DNA-photodamaging properties (12).

MATERIALS AND METHODS

Materials. The synthesis and structural identification of the thienocarbazoles (TCL and TCA) and the nitro-precursors (2mPTC and 3mPTC) have been described previously (9). The complete systematic nomenclature and abbreviations for the compounds studied are as follows—TCL: 2,3,4,10-tetramethyl-5*H*-thieno[3,2-*b*]carbazole for the linear thienocarbazole; TCA: 2,3,5-trimetyl-10*H*-thieno[2,3-a]carbazole for the angular thienocarbazole; 2mPTC: 5-(2′-nitrophenyl)-2,3-dimethylbenzo[*b*]thiophene for the dimethyl thienocarbazole precursor; 3mPTC: 6-(2′-nitrophenyl)-2,3,7-trimethylbenzo[*b*]thiophene for the trimethyl thienocarbazole precursor.

The match of the excitation with the absorption spectra, together with the elemental analysis data, attested the purity of the compounds.

Elemental analysis for the thienocarbazoles—TCA, $C_{17}H_{15}NS$: calcd C 76.9, H 5.7, N 5.3, S 12.1; found C 76.7, H 5.5, N 5.2, S 12.0 and TCL, $C_{18}H_{17}NS$: calcd C 77.5, H 6.4, N 5.3, S 11.6; found C 77.7, H 6.5, N 5.2, S 11.6.

CBZ (Aldrich Gold Label) and TN (Lancaster Synthesis 98+%) were used as received.

Solvents were of spectroscopic or equivalent grade. Concentrations of solutions were in the range from 10^{-6} to 1×10^{-5} *M*. These were deoxygenated by bubbling with nitrogen or argon. Ethanol was dried over CaO, and 1,4-dioxane was purified by the procedure described in Seixas de Melo *et al.* (13).

Measurements. Absorption and luminescence spectra were recorded on Shimadzu UV-2100, Olis-Cary 14 and Jobin-Ivon SPEX Fluorolog 3-22 spectrometers. For phosphorescence a 1934 D phosphorimeter accessory was used. Fluorescence and phosphorescence spectra were corrected for the wavelength response of the system.

Fluorescence quantum yields were measured using α-terthienyl in ethanol as a standard ($\phi_F = 0.054$) (14). The fluorescence quantum yields at 77 K were obtained by comparison of the spectra at this temperature and at 293 K run under the same experimental conditions, and the ϕ_F value was calculated assuming that the sample volume ratio $V_{293K}/V_{77K} = 0.8$ (15).

Phosphorescence quantum yields were obtained using benzophenone in ethanol as a standard ($\phi_{Ph} = 0.84$) (15).

The molar extinction coefficients (ε) were obtained at absorption maxima from the slope of the plot of the absorption with seven solutions of different concentrations *vs* the concentration (correlation values ⩾0.999).

Triplet–singlet difference absorption spectra and yields were obtained using an Applied Photophysics laser flash photolysis equipment pumped by an Nd:YAG laser (Spectra Physics, Mountain View, CA) with an excitation wavelength of 355 or 266 nm (16,17). First-order kinetics was observed for the decay of the lowest triplet state. The transient spectra (300–700 nm) were obtained by monitoring the optical density (OD) change at 5–10 nm intervals, averaging at least 10 decays at each wavelength.

In all cases the signal was assigned to a triplet state because (1) it was quenched by oxygen (quenching constant by oxygen, $k_{ox} = 9.3 \times 10^9$ $M^{-1}\cdot s^{-1}$ for TCA and $k_{ox} = 5 \times 10^9$ $M^{-1}\cdot s^{-1}$ for TCL); (2) it decayed by first-order kinetics with microsecond lifetimes; and (3) other possible transients, such as radical ions, generally are not produced on photolysis in the nonpolar solvent benzene.

The triplet molar absorption coefficients of TCL and TCA in benzene were determined by the singlet depletion technique according to the well-known relationship (18)

$$\varepsilon_T = \frac{\varepsilon_S \Delta OD_T}{\Delta OD_S} \tag{1}$$

where both ΔOD_S and ΔOD_T are obtained from the triplet transient absorption spectra, and triplet formation quantum yields are derived from these and by actinometry with benzophenone. The ϕ_T values were obtained by comparing the ΔOD at 525 nm of a benzene solution of benzophenone (the standard) with that of the compound (optically matched at the laser wavelength) using the following equation (19):

$$\phi_T^{TCL} = \frac{\varepsilon_{TT}^{Benzophenone}}{\varepsilon_{TT}^{TCL}} \frac{\Delta OD_{max}^{TCL}}{\Delta OD_{max}^{Benzoph}} \phi_T^{Benzophenone} \tag{2}$$

The ϕ_T value for TCL was consequently obtained by using Eq. 2, with $\varepsilon_{TT}^{Benzophenone} = 7200$ $M^{-1}\cdot cm^{-1}$, $\phi_T^{Benzophenone} = 1$ and $\varepsilon_{TT}^{TCL} = 27100$ $M^{-1}\cdot cm^{-1}$ (obtained with Eq. 1).

In the case of TCA the triplet formation quantum yield was determined by measuring the enhancement of triplet population promoted by *N,N*-bromodimethylaniline (BrDMA) (20). The effects promoted by BrDMA on both ϕ_F and triplet generation (which is proportional to the absorbance change ΔA) can be taken into account using the following equation (20,21):

$$\frac{\phi_F^0}{\phi_F} - 1 = \phi_T \left(\frac{\phi_F}{\phi_F^0} \frac{\Delta A^0}{\Delta A} - 1 \right) \tag{3}$$

where ϕ_F^0 and ΔA^0 refer to these quantities without BrDMA, whereas ϕ_F and ΔA refer to the solutions in the presence of different amine concentrations. From a plot of $\phi_F^0/\phi_F - 1$ *vs* $\phi_F \Delta A^0/\phi_F^0 \Delta A - 1$, ϕ_T is obtained with an experimental error of ±15%.

The time-resolved photoacoustic calorimetry (PAC) apparatus was described in detail elsewhere (4,13). Briefly, the PAC cell follows the front-face design with a dielectric mirror protecting the transducer from the light impinging on the cell (22). The sample and reference solutions flow at a rate of 1 mL·min^{-1} through a 0.11 mm thick cell, where they are irradiated with an unfocused Photon Technology International (PTI) dye laser (model PL2300), pumped by a N_2 laser working at a frequency of 2 Hz, or directly with the N_2 laser. The thienocarbazoles TCL and TCA were irradiated at an excitation wavelength of λ_{exc} = 337 nm. In a typical PAC experiment we first match the absorbances of the reference (2-hydroxybenzophenone) and sample solutions at the excitation wavelength. The absorbances of the solutions used were 0.15, in a standard 1 cm quartz cuvette, at the excitation wavelength. Then, with a continuous flow of the solutions (flow rate of 1 mL·min^{-1}), 100 acoustic waves of the sample, reference and pure solvent are collected and averaged under the same experimental conditions. Four sets of averaged sample, reference, and solvent waves are used for data analysis at a given laser intensity, and four laser intensities are used in each experiment. The different laser intensities are obtained by interposing neutral density filters with transmissions in the 30–100% range (79%, 57.7% and 32.6% when using λ_{exc} = 337 nm). For the $\phi_T E_T$ determinations (where ϕ_T stands for the $S_1 \sim\!\!\rightarrow T_1$ ISC yield, and E_T is the energy of the 0–0 level taken from the onset of the phosphorescence spectra), all the sample, reference and solvent solutions were deaerated by continuously bubbling N_2 during the course of the experiment, thereby ensuring that all the samples were kept continuously free of O_2. For ϕ_Δ determinations air-saturated solutions were used.

The pure solvent signal was scaled by the fraction of light absorbed by the sample in the PAC cell (typically 5%) and subtracted from the sample and reference signals before data analysis. We used the Marquardt program previously described (23,24) to deconvolute the sample and reference signals. The PAC references were chosen because they convert all the light energy absorbed into thermal energy in a time much shorter than the transducer oscillation frequency (2.25 MHz).

Fluorescence decays were measured using a home-built time-correlated single-photon counting (TCSPC) apparatus with a N_2-filled IBH 5000 coaxial flashlamp as excitation source, a Jobin-Ivon monochromator, a Philips XP2020Q photomultiplier and a Canberra Instruments time-to-amplitude converter and multichannel analyzer. Alternate measurements (1000 counts per cycle), controlled by Decay® software (Biodinâmica, Lisbon, Portugal), of the pulse profile at 285, 337 or 356 nm and the sample emission were taken until 1–2 × 10^4 counts at the maximum were reached (10). The fluorescence decays were analyzed using the modulating functions method of Striker *et al.* (25) with automatic correction for the photomultiplier "wavelength shift."

Semiempirical calculations. Quantum mechanical–molecular orbital calculations were performed on a Silicon Graphics Inc. O2 workstation using the Cerius-2 (from Molecular Simulations Incorporated [MSI], San Diego, CA) software. Geometry optimization and transition energies were calculated using the Austin Model 1 with configuration interaction (AM1-CI) (26) level included in the MOPAC6.0 version. Hyperchem software (release 6.01 for Windows) was used to obtain transition energies and oscillator strengths by means of the Zerner intermediate neglect of differential overlap/spectroscopy with configuration interaction (ZINDO/S-CI) technique (27).

Geometries were first optimized at the AM1 level, and these were used to perform the CI calculation. The geometry obtained was then introduced as input data for the ZINDO/S-CI method. For the AM1 calculation single- and double-configuration interaction (CI) was used, involving 100 (five highest occupied molecular orbitals [HOMO] and five lowest unoccupied molecular orbitals [LUMO]) configurations. For ZINDO/S-CI, in which the configuration interactions (CI) extended to 10 occupied and 10 unoccupied molecular orbitals, only the singly excited configurations were allowed, leading to 201 singly excited configurations. For the ZINDO method the overlap-weighting factors used were 1.267 for sigma–sigma orbitals and 0.585 for pi–pi orbitals (28,29).

RESULTS

Figure 1 shows the absorption spectra of the thienocarbazoles TCA and TCL and of their nitro-precursors 2mPTC and 3mPTC. With TCA and TCL three major bands are observed in the UV spectra, corresponding to the $S_0 \rightarrow S_1$, $S_0 \rightarrow S_2$ and $S_0 \rightarrow S_3$ transitions. In the thienocarbazoles there is a clear redshift of the longer-wavelength–absorbing band of the TCL relative to the TCA. Similarities are observed between these and the UV spectra of the nitro-precursors, except that with 3mPTC an additional band occurs in the 280–320 nm region. With 2mPTC this band is not observed, but the lower-wavelength band at 260 nm is redshifted relative to the 3mPTC compound.

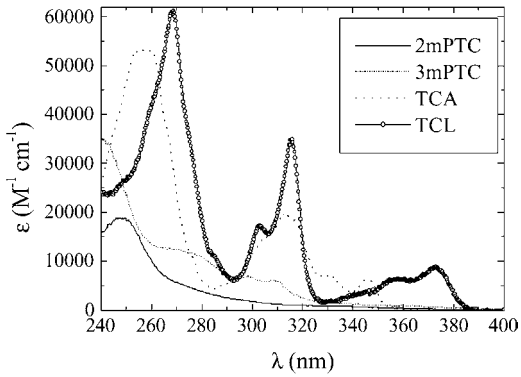

Figure 1. Absorption spectra of 2mPTC (5.6×10^{-5} *M*), 3mPTC (1.97×10^{-5} *M*), TCA (6.96×10^{-6} *M*) and TCL (9.80×10^{-6} *M*) in ethanol at T = 293 K.

Figure 2 shows the fluorescence emission spectra of all the four compounds at RT. The spectra at low temperature (LT) also are shown for TCA and TCL. On going from RT to LT blueshifts, an increase in vibrational resolution is observed. With the nitro-precursors no significant changes were observed (spectra not shown). Again, as observed in the case of the absorption spectra, the maximum fluorescence of the compound TCL also is redshifted, now by ≈30 nm relative to TCA.

Figure 3 shows the phosphorescence spectra in ethanol of the four compounds studied. As observed for absorption and fluorescence, the phosphorescence spectra of TCL are redshifted relative to TCA. With the precursors the less methylated compound 2mPTC shows a blueshift relative to the more methylated 3mPTC. This behavior is similar to that observed in the fluorescence spectra of these compounds (see Fig. 2).

Figure 4 presents the transient triplet–singlet difference absorption spectra of TCA and TCL, and the spectral and photophysical data of all compounds are summarized in Table 1.

DISCUSSION

Spectral and photophysical properties of the nitro-precursors 2mPTC and 3mPTC

The low values obtained for the ϕ_F and ϕ_{Ph} values of the precursors 2mPTC and 3mPTC are consistent with the non-radiative decay processes ($S_1 \sim\!\!\rightarrow S_0$ internal conversion and $T_1 \sim\!\!\rightarrow S_0$ intersystem crossing [ISC]) being the preferred deactivation channels in these compounds. This also is reflected in the comparison of their radiation-less (k_{NR}) and radiative rate constants (see Table 1). Although their fluorescence yields are identical, the same is not true for the fluorescence lifetimes, with the less methylated 2mPTC having a value *ca* 16 times larger than that of 3mPTC. However, the possible existence of a major decay component, with a decay time lower than 200 ps (the time

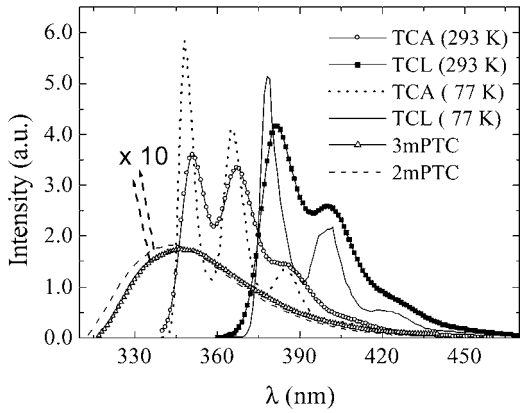

Figure 2. Fluorescence emission spectra of TCA (3.48×10^{-6} *M*), TCL (3.77×10^{-6} *M*), 2mPTC (6.22×10^{-5} *M*) and 3mPTC (1.25×10^{-5} *M*) in ethanol. The spectra of the last two compounds are magnified by a factor of 10.

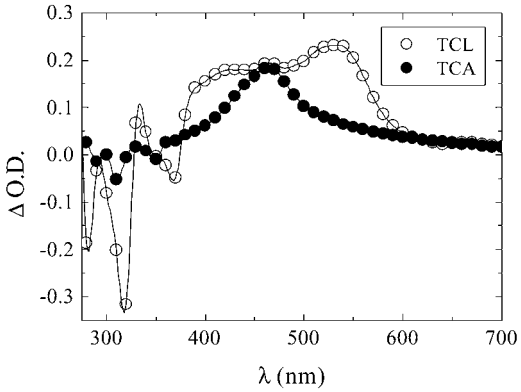

Figure 4. Transient absorption spectra of TCL (9.43×10^{-6} *M*) and TCA (8.70×10^{-6} *M*) in benzene at T = 298 K; delay after flash is 1 μs for TCL and 0.1 μs for TCA.

resolution of our TCSPC equipment is 200 ps [10]), should be considered. Although this influences the absolute value of the radiative rate constant, in practical terms it does not affect the balance between this and the k_{NR} value. The introduction of nitro groups in benzene derivatives is known to redshift the 200 nm benzene ring and, in addition, introduces strong vibrational couplings that lead to emission quenching (30).

Based on the experimental values for the radiative rate constants and low extinction coefficients of the lowest transition (Table 1, Fig. 1), the lowest-lying singlet excited state for these two compounds is of n,π* origin. Although from the k_F value for 2mPTC, S_1 could be assigned to a π,π* state, theory predicts that it is n,π*, and this is supported by the fact that there are no other significant differences between the two compounds. Predicted and experimental spectral data are compared in Tables 1 and 2.

Assignment of triplet state configurations is based on (1) the relatively large gap, ΔE_{ST}, between the lowest singlet and emitting triplet when T_1 is π,π*; and (2) the characteristic phosphorescence lifetimes ($\tau_{Ph} < 0.01$ s for n,π* states and of seconds for π,π* states) (31). The long phosphorescence lifetimes observed for the compounds (0.35 and 0.45 s, see Table 1) indicate that emission is from a triplet π,π* state (10,31). This is supported by the relatively large S_1–T_1 energy gap observed (≈6000 cm^{-1}), which again is characteristic of a $^3(\pi,\pi^*)$ state (10,31). Smaller ΔE_{ST} values are normally observed with $^3(n,\pi^*)$ states (31). This suggests that an additional triplet of n,π* origin exists between S_1 and T_1 and could be responsible for the low triplet yield value (within the experimental conditions used, no triplet signal was observed in solution by flash photolysis for the compounds 2mPTC and 3mPCT, which most probably means that $\phi_T \leqslant 0.01$). This, together with the very efficient radiation-less deactivation pathway between T_1 and S_0, explains the low phosphorescence yield of these compounds. With these precursors a degree of rotational freedom exists between the nitrobenzene and thianapthene rings. This significant inter-ring bond torsional coupling is likely to result in a large radiation-less rate constant for the $T_1 \sim\sim\rightarrow S_0$ process, leading to marked quenching of the phosphorescence emission.

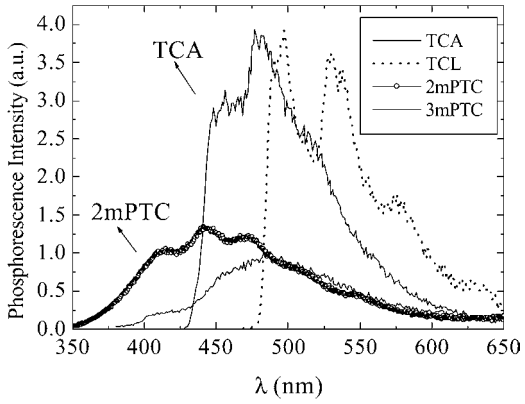

Figure 3. Phosphorescence spectra of TCA, TCL, 2mPTC and 3mPTC in ethanol. Concentrations of the compounds are identical to those in Fig. 2.

Spectral and photophysical properties for the thienocarbazoles TCA and TCL

The ring closure of the nitro-precursors to thienocarbazoles leads, first, to a strong redshift of the longer-wavelength–absorbing bands (see Fig. 1). These redshifts of TCL and TCA relative to their precursors also are observed in fluorescence and phosphorescence (Figs. 2 and 3) and are a direct consequence of the increase in the π-electron path, with subsequent decrease in the energetic difference between the HOMO and the LUMO (31,32). In addition, in the absorption spectra of TCL and TCA, three clearly defined bands are observed, with the two longest wavelengths also displaying vibrational resolution. Comparison between the thienocarbazoles and their nitro-precursors also shows that the radiative parameters (ϕ_F, τ_F, ϕ_{Ph}) are all greater for the former, and the radiative rate constants now display typical values for allowed π,π* transitions. This assignment is supported by the high values of the extinction coefficients for both TCA and TCL (see Fig. 1). It is also relevant that there is no change in the ϕ_F value from RT to LT, indicating that no structural change is expected to occur. In addition, this also confirms that the sum $\phi_F + \phi_T$ is ≈1 because if internal conversion (IC) were operative, an increase in the competitive fluorescence quantum yield would have been expected from 293 to 77 K. However, although the two compounds show similar photophysical behavior, the same is not true for their spectroscopic characteristics such as absorption, fluorescence and phosphorescence maxima, where the bands in TCL are all

Table 1. Spectroscopic and photophysical data for the compounds studied in ethanol. Also shown are the same properties for the CBZ and TN compounds*

	λ_{max} (nm) ($S_0 \rightarrow S_n$)	E_{0-0}† (cm^{-1}) ($S_1 \rightarrow S_0$) (293 K)	E_{0-0}† (cm^{-1}) ($S_1 \rightarrow S_0$) (77 K)	E_{0-0}‡ (cm^{-1}) ($T_1 \rightarrow S_0$)	ϕ_F (293 K)	ϕ_F (77 K)	τ_F (ns)	ϕ_{Ph}	τ_{Ph} (s)	τ_T (μs)	ϕ_T	ϕ_Δ	S_Δ	k_F§ (ns^{-1})	k_{NR}§ (ns^{-1})	k_{ISC}§ (ns^{-1})	k_{IC}§ (ns^{-1})
2mPTC	<u>248</u> 325	31 546	—	27 933	0.0033	—	3.62‖	0.009	0.45	—	—			0.0009	0.275	—	—
3mPTC	<u>240</u> 267 330	32 050	—	25 253	0.0032	—	0.22	0.004	0.35	—	—			0.0145	4.531	—	—
TCA	<u>257</u> 346	28 736	28 830	23 256	0.057	0.058	1.08	0.154	0.64	4	0.94¶ 0.95#	0.35	0.37	0.053	0.873	0.87 0.88	0.003 ≅0
TCL	<u>269</u> 372	26 525	26 596	20 833	0.086	0.081	1.52	0.073	0.45	12	0.34** 0.84#	0.32	0.94 0.38	0.057	0.601	0.224 0.55	0.377 0.05
CBZ	<u>255</u> 337 376	30 121	29 499	24 631	0.41	0.44 (15)	12.4	0.24 (15)	6.8 (15)	—	0.36 (15)	—	—	0.033	0.048	0.03	0.02
TN	<u>228</u> 297	33 670	33 784	24 096	0.019	0.021	0.28	0.44	0.31	3	0.98 (15)	—	—	0.069	3.5	3.5	≅0

*The underlined values represent the maxima in the spectra.
†0–0 energies obtained from the overlap point of normalized absorption and fluorescence spectra, with the exception of 2mPTC and 3mPTC, where data were taken from the onset of the emission band.
‡Obtained from the onset of the phosphorescence spectra.
§$k_F = \frac{\phi_F}{\tau_F}$; $k_{NR} = \frac{1-\phi_F}{\tau_F}$; $k_{ISC} = \frac{\phi_T}{\tau_F}$; $k_{IC} = \frac{1-\phi_F-\phi_T}{\tau_F}$. ϕ_F and ground-state extinction coefficient determinations with associated errors of ±5%; ϕ_T determinations with associated errors of ±15%.
‖The time resolution of our TCSPC was 200 ps; see text for more details.
¶Value obtained by measuring the enhancement of triplet population promoted by BrDMA.
#Value obtained by PAC.
**Value obtained by the singlet-depletion method.

redshifted relative to TCA (Table 1, Figs. 1–4), suggesting less conjugation in the angular TCA. This loss in π-electron conjugation of TCA relative to TCL also may have implications for the triplet properties as will be discussed below.

Contrary to the ϕ_T determination for TCL, where the singlet depletion technique could be used, in the case of TCA there is strong evidence for triplet–triplet absorption in the singlet region. In fact, it can be seen from Fig. 4 that the maxima obtained in the depletion region are not coincident with those found for singlet–singlet absorption (Fig. 1). This strongly suggests triplet–triplet absorption in that region. Consequently, the ϕ_T value for TCA was first obtained by measuring the enhancement of triplet population promoted by BrDMA (20) (Fig. 5).

The use of two different techniques to obtain ϕ_T values should, however, be considered with caution. In the particular case of TCL the obtained value is strongly dependent on the assumption that the nascent triplet does not absorb in the spectral region where singlet depletion is observed. The obtained ε_T (from Eq. 1) is consequently an upper limit, and thus ϕ_T (from Eq. 2) should be considered as a lower limit. Moreover, in the case of TCA, although there is clear evidence for transient triplet absorption in the singlet depletion region, we have used the same singlet depletion method to obtain a lower value for ϕ_T. The value obtained for ε_T (TCA) was 20 250 $M^{-1}\cdot cm^{-1}$. With the actinometer benzophenone the obtained ϕ_T value for TCA (Eq. 2) was 0.56 (lower limit). To obtain more accurate singlet–triplet ISC yields, PAC was used as an alternative method.

The time-resolved PAC technique gives the fraction of heat released in nonradiative processes as well as the decay times associated with such processes. In the present case the fractions of heat released can be conveniently divided into a fast and a slow step, ϕ_1 and ϕ_2, with associated lifetimes τ_1 and τ_2, respectively. The fast step has a lifetime shorter than or close to 1 ns ($\tau_1 \leqslant 1$ ns) and includes the internal conversion from S_n to S_1, the internal conversion from S_1 to S_0, the ISC to the triplet manifold (ϕ_{ISC}) and the relaxation of the spectroscopically formed ground state species (see Scheme 2). The triplet lifetime exceeds the time resolution of the 2.25 MHz transducer used in these PAC experiments (see τ_T values in Table 1) and gives a meaningless fraction of energy released, $\phi_2(N_2)$ (13,33). Consequently, the only relevant value in the deconvolution procedure is ϕ_1. The thermal energy released in the fast step, associated with τ_1 and caused by the formation of the relaxed S_1 state, followed by the formation of the triplet state (ϕ_T) and by internal conversion to the ground state, is therefore given by (13,33)

$$\phi_1 E_{hv} = (E_{hv} - E_{S_1}) + E_{S_1}\phi_{IC} + (E_{S_1} - E_{T_1})\phi_T + \Delta E_r \phi_F \quad (4)$$

The last term in Eq. 4 is related to the contribution of the ground state species relaxation, within the studied time window, to the thermal energy dissipated in the lifetime τ_1 (13). The energy of S_1, E_{S_1}, is therefore a joint contribution of the relaxation term plus the energy of fluorescence given by $E_{\bar{v}\,max}$ (the energy at the maximum

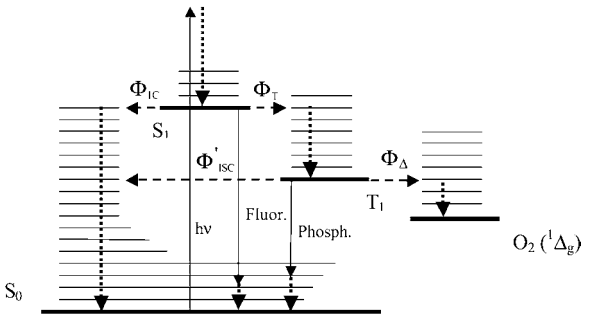

Scheme 2.

Table 2. Experimental (exp.) and theoretical (theor.) data for the first two lowest transition energies ($S_{1,2} \leftarrow S_0$) and oscillator strength (f) for the compounds studied obtained by the ZINDO/S method

Compound	Transition	λ(nm) (ZINDO-CI/S)	f (theor.)	λ_{max} (nm) (exp.)	ε (M^{-1}·cm^{-1})	Δλ (exp. − theor.)
2mPTC	$S_0 \rightarrow S_2$	241	0.4185	248	18 900	7
	$S_0 \rightarrow S_1$	364	0.0004	325	990	−39
3mPTC	$S_0 \rightarrow S_2$	222	0.2151	240	22 540	18
	$S_0 \rightarrow S_1$	413	0.0002	330	1230	−83
TCA	$S_0 \rightarrow S_3$	257	0.0447	257	53 530	0
	$S_0 \rightarrow S_2$	297	0.051	313		16
	$S_0 \rightarrow S_1$	343	0.3273	346	6350	3
TCL	$S_0 \rightarrow S_3$	325	0.7588	269	61 630	−56
	$S_0 \rightarrow S_2$	351	0.0812	315		−36
	$S_0 \rightarrow S_1$	371	0.0001	372	6310	1

fluorescence intensity taken as the Gaussian center of the fluorescence band): $E_{S_1} = E_{\bar{\nu}\,max} + \Delta E_r$ (13).

In degassed solutions the development of this expression leads to (13)

$$\phi_T E_T = (1 - \phi_1)E_{hv} - \phi_F E_{\bar{\nu}\,max} \quad (5)$$

From Eq. 5 we obtain the product $\phi_T E_T$, and consequently the triplet quantum yield can be obtained only if the triplet energy is known. From the onset of the phosphorescence bands, we have used the values 2.88 eV (430 nm) and 2.58 eV (480 nm) for the E_T values of TCA and TCL, respectively (see Table 1, Fig. 3). Taking E_{hv} = 3.68 eV and with the obtained ϕ_1 = 0.1993 and 0.3345 values for TCA and TCL, respectively, Eq. 5 leads to ISC yields of 0.95 ± 0.005 for the former and 0.84 ± 0.04 for the latter. As a consequence of all of the above, there is clear evidence of triplet contamination in the singlet depletion region for both TCA and TCL. In the case of TCA there is a perfect match between the result of this determination and that obtained by measuring the enhancement of triplet population promoted by BrDMA, thus giving full confidence in this value, whereas in the case of TCL there is a clear disagreement between the values obtained by the two independent methods. The PAC method is clearly more sensitive but has the disadvantage resulting from the fact that the ϕ_T value, obtained from Eq. 5, depends on the fraction of heat released (PAC experiment) and on the other three independent measurements or techniques (fluorescence, phosphorescence and flash photolysis). The resulting ϕ_T value will obviously be the result of all the associated errors of the experiments. However, previous use of PAC techniques to obtain ϕ_T (4,33,34) and E_T (13,34,35) values have shown great accuracy, portending its use for such determinations. An illustrative example of photoacoustic waves is presented in Fig. 6 for TCL in benzene solution.

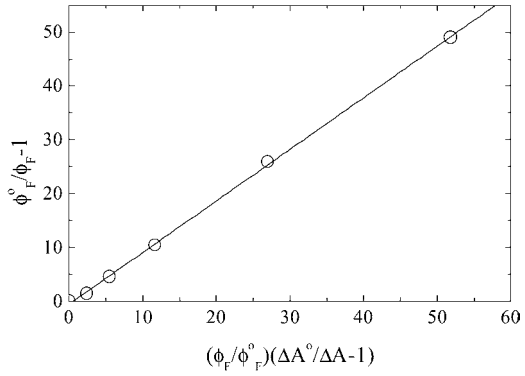

Figure 5. Experimental data plotted according to Eq. 3, thus translating the effects promoted by BrDMA on both ϕ_F and ΔA for TCA (6.96×10^{-6} *M*).

The determinations of ϕ_Δ values with the PAC technique imply the use of air-saturated solutions. In this case ϕ_2 (air) is associated with the transfer of energy from the triplet state of the sensitizer to molecular oxygen (see Scheme 2). The decay time associated with this fraction of heat released, τ_2, is established with flash photolysis experiments using air-containing solutions ($\tau_2 \approx 50$ ns for both TCA and TCL) and is maintained unchanged in the deconvolution procedure of the PAC waves, together with the τ_1 value (again $\leqslant$ 1 ns). In these air-saturated solutions ϕ_Δ can be obtained from the fraction of heat released (ϕ_2 in Scheme 2) in the formation of the singlet oxygen from the triplet state of the thienocarbazole. The energy released in the slow thermal process, associated with τ_2, is now due to the decay of the triplet state to give singlet oxygen (with quantum yield ϕ_Δ) and to its return to the ground state (quantum yield ϕ'_{ISC} in Scheme 2) (4,33)

$$\phi_2 E_{hv} = (E_T - E_D)\phi_\Delta + \phi'_{ISC} E_T$$

and, thus, considering that $\phi_\Delta + \phi'_{ISC} = \phi_T$, we finally obtain

$$\phi_\Delta = \phi_T S_D = \frac{\phi_T E_T - E_{hv}\phi_2}{E_\Delta}$$

where S_Δ accounts for the efficiency of triplet energy transfer to produce singlet oxygen. Using the value of E_Δ = 0.974 eV and with the ϕ_T values obtained from the PAC experiments, we have obtained the ϕ_Δ values presented in Table 1. In general, the ϕ_Δ and S_Δ values obtained revealed *ca* 30–40% efficiency to produce $^1O_2$. These can be considered moderate efficiencies and potentially suggest that additional structural modifications should be attempted to increase those values.

An interesting observation from the photophysics of these compounds is the differences obtained in their ISC yields. If we consider the more reliable ϕ_T values, obtained from PAC, in Table 1, it can be seen that the linear compound has a ϕ_T value lower (0.84) than that obtained for the angular compound (0.94). The difference is not that much significant, but it is legitimate to think that TCL has a lower value than does TCA because both values were obtained with the same technique. The explanation for this difference can be found when their CBZ and TN counterparts are compared, where TN has a ϕ_T value of 0.98, whereas for CBZ this value is 0.36 (see Table 1). Comparison between these suggests that in the case of the angular compound a disconnection between the two CBZ and TN ring systems is induced, with the latter unit

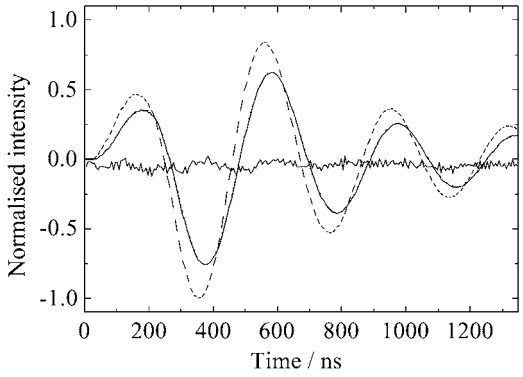

Figure 6. Photoacoustic waves for TCL (6.6×10^{-5} *M*) in benzene solution. The reference (T-wave, dash), sample (E-wave, solid) and calculated waves (C-wave, dot) are shown. Also shown are the residuals, (C-wave) − (E-wave) × 10 (dash–dot). The calculated wave was obtained with two sequential decays, with the first lifetime fixed at 1.52 ns. See text for more details.

having a higher ϕ_T value that dominates ISC in TCA, whereas in the case of the TCL there is only a partial decoupling. This is not the case, however, with the phosphorescence quantum yields, where the individual chromophores (TN and CBZ) possess higher values than do the thienocarbazoles. Nevertheless, with the phosphorescence spectra, similarities are observed between TCA and the nitro-precursor 3mPTC (note that both compounds have three methyl groups). In fact, their phosphorescence maxima are practically identical (Fig. 2), and the shapes of their bands are fairly similar, which again supports the idea that there is a partial decoupling between the benzothiophene ring system and the CBZ unit (or indole if we ignore the middle benzene ring shared between the two units) in the angular compound, with the π-electron path responsible for the phosphorescence (T_1 state) being essentially located in the TN ring.

Note also that in contrast to what was observed with the precursors, with TCA and TCL the sum $\phi_T + \phi_F \approx 0.9–1$, showing negligible deactivation by internal conversion. Comparison of the thienocarbazoles with their benzothiophene-substituted nitrobenzene derivatives shows that although with the latter the nonradiative processes control the photophysics of the compounds, in the case of the former the contribution of the nonradiative processes from S_1 to S_0 is negligible.

The semiempirical ZINDO/S-CI calculation method predicts reasonably well the transition energies of the compounds studied, except perhaps for the longer-wavelength absorption for 3mPTC. With the nitro-precursors the oscillator strength values are clearly consistent with the low extinction coefficient values obtained for the longer-wavelength transition. Theory also predicts these transitions to be of n,π* origin, which is in agreement with the experimental observations. In the case of the thienocarbazoles there is almost perfect agreement between the experimental and theoretical data in the case of TCA, whereas with TCL there is some inconsistency with the relative intensities of the three bands. Further, with these, theory predicts that all the transition states are π,π* in nature and that the longer-wavelength transition is redshifted in TCL relative to TCA. To obtain more accurate values, higher levels of calculation and sophistication are required, which clearly was not the aim of the present work. With the nitro-precursors the dependence of the above values (transition energies and oscillator strengths) with the angle of torsion between the benzothiophene and the nitrobenzene rings was not explored. However, in analogous molecules this has been demonstrated to affect these parameters strongly (10).

CONCLUSIONS

We have accomplished a complete spectroscopic and photophysical study of two new thienocarbazoles and their synthetic nitro-precursors. The position of the CBZ ring (relative to the thiophene ring) has been shown to change the spectroscopic characteristics of the compounds, thus inducing a redshift of the singlet and triplet absorption, and fluorescence and phosphorescence wavelength maxima for TCL relative to TCA. The fluorescence properties of both compounds are identical, whereas their triplet yields are slightly different. It was established that this is a consequence of the predominance of the TN ring in the angular compounds compared with the linear compound. The thienocarbazoles studied here belong to a category of photosensitizers that are potentially useful in various applications. In fact, their high triplet yields and microsecond triplet lifetimes suggest potential photoactive action. The singlet oxygen yields obtained for the thienocarbazoles reveal a potential for photosensitization activity, although the efficiency of triplet energy transfer to produce singlet oxygen is low, and the development of new synthetic derivatives should be pursued. Based on experimental data and comparison with theory, the S_1 and T_1 states of TCA and TCL are predicted to be π,π*, whereas for the precursors S_1 is n,π*.

Acknowledgement—Financial support from Fundação para a Ciência e a Tecnologia (FCT) is acknowledged.

REFERENCES

1. Spikes, J. D. (1989) Photosensitization. In *The Science of Photobiology* (Edited by K. C. Smith), pp. 79–110. Plenum Press, New York.
2. Bensasson, R. V., E. J. Land and T. G. Truscott (1993) *Excited States and Free Radicals in Biology and Medicine. Contributions from Flash Photolysis and Pulse Radiolysis*. Oxford Science Publications, New York.
3. Spikes, J. D. (1986) Phtalocyanines as photosensitizers in biological systems and for the photodynamic therapy of tumors. *Photochem. Photobiol.* **43**, 691–700.
4. Pineiro, M., A. L. Carvalho, M. M. Pereira, A. M. d. A. R. Gonsalves, L. G. Arnaut and S. J. Formosinho (1998) Photoacoustic measurements of porphyrin triplet-state quantum yields and singlet-oxygen efficiencies. *Chem. Eur. J.* **4**, 2299–2307.
5. Pineiro, M., M. M. Pereira, A. M. d. A. Rocha Gonsalves, L. G. Arnaut and S. J. Formosinho (2001) Singlet oxygen quantum yields from halogenated chlorins: potential new photodynamic therapy agents. *J. Photochem. Photobiol. A: Chem.* **138**, 147–157.
6. Dalton, L. K., S. Demerac, B. C. Elmes, J. W. Loder, J. M. Swan and T. Teitei (1967) Synthesis of tumour-inhibitory alkaloids ellipticine 9-methoxyellipticine and related pyrido[4,3-b]carbazoles. *Aust. J. Chem.* **20**, 2715–2727.
7. Ferreira, I. C. F. R., M.-J. R. P. Queiroz and G. Kirsch (2002) Novel synthetic routes to thienocarbazoles via palladium or copper catalyzed amination or amidation of arylhalides and intramolecular cyclization. *Tetrahedron* **58**, 7943–7949.
8. Rosseau-Richard, C., C. Auclair, C. Richard and R. Martin (1990) Free-radical scavenging and cytotoxic properties in the ellipticine series. *Free Radic. Biol. Med.* **8**, 223–230.
9. Ferreira, I. C. F. R., M.-J. R. P. Queiroz and G. Kirsch (2001) Synthesis of new methylated thieno[2,3-a] and [3,2-b]carbazoles by reductive cyclization of 6-(2′-nitrophenyl)benzo[b]thiophenes obtained by palladium-catalyzed cross-coupling. *J. Heterocycl. Chem.* **38**, 749–754.
10. Seixas de Melo, J. and P. F. Fernandes (2001) Spectroscopy and photophysics of 4- and 7-hydroxycoumarins and their thione analogs. *J. Mol. Struct.* **565/566**, 69–78.
11. Ostrovidov, S., P. Franck, D. Joseph, L. Martarello, G. Kirsch, F.

Belleville, P. Nabet and B. Dousset (2000) Screening of new antioxidant molecules using flow cytometry. *J. Med. Chem.* **43**, 1762–1769.
12. Ihmels, H., K. Faulhaber, K. Wissel, G. Bringmann, K. Messer, G. Viola and D. Vedaldi (2001) Synthesis and investigation of the DNA-binding and DNA-photodamaging properties of indolo 2,3-b quinolizinium bromide. *Eur. J. Org. Chem.* 1157–1161.
13. Seixas de Melo, J., L. M. Silva, L. G. Arnaut and R. S. Becker (1999) Singlet and triplet energies of alpha-oligothiophenes: a spectroscopic, theoretical, and photoacoustic study: extrapolation to polythiophene. *J. Chem. Phys.* **111**, 5427–5433.
14. Becker, R. S., J. Seixas de Melo, A. L. Maçanita and F. Elisei (1996) Comprehensive evaluation of the absorption, photophysical, energy transfer, structural, and theoretical properties of alpha-oligothiophenes with one to seven rings. *J. Phys. Chem.* **100**, 18683–18695.
15. Murov, S., I. Charmichael and G. L. Hug (1993) *Handbook of Photochemistry*. M. Dekker, New York.
16. Seixas de Melo, J., F. Elisei, C. Gartner, G. G. Aloisi and R. S. Becker (2000) Comprehensive investigation of the photophysical behavior of oligopolyfurans. *J. Phys. Chem. A* **104**, 6907–6911.
17. Seixas de Melo, J., L. M. Silva and M. Kuroda (2001) Photophysical and theoretical studies of naphthalene-substituted oligothiophenes. *J. Chem. Phys.* **115**, 5625–5636.
18. Carmichael, I. and G. L. Hug (1986) Triplet-triplet absorption-spectra of organic-molecules in condensed phases. *J. Phys. Chem. Ref. Data* **15**, 1–250.
19. Kumar, C. V., L. Qin and P. K. Das (1984) Aromatic thioketone triplets and their quenching behavior towards oxygen and di-t-butylnitroxy radical. A laser-flash-photolysis study. *J. Chem. Soc. Faraday Trans. 2* **80**, 783–793.
20. Medinger, T. and F. Wilkinson (1965) Mechanism of fluorescence quenching in solution. I. Quenching by bromobenzene. *Trans. Faraday Soc.* **61**, 620–630.
21. Seixas de Melo, J., R. S. Becker, F. Elisei and A. L. Maçanita (1997) The photophysical behavior of 3-chloro-7-methoxy-4-methylcoumarin related to the energy separation of the two lowest-lying singlet excited states. *J. Chem. Phys.* **107**, 6062–6069.
22. Arnaut, L. G., R. A. Caldwell, J. E. Elbert and L. A. Melton (1992) Recent advances in photoacoustic calorimetry—theoretical basis and improvements in experimental-design. *Rev. Sci. Instrum.* **63**, 5381–5389.
23. Ni, T., R. A. Caldwell and L. A. Melton (1989) The relaxed and spectroscopic energies of olefin triplets. *J. Am. Chem. Soc.* **111**, 457–464.
24. Melton, L. A., T. Q. Ni and Q. Z. Lu (1989) Photoacoustic calorimetry—a new cell design and improved analysis algorithms. *Rev. Sci. Instrum.* **60**, 3217–3223.
25. Stricker, G., V. Subramaniam, C. A. M. Seidel and A. Volkmer (1999) Photochromicity and fluorescence lifetimes of green fluorescent protein. *J. Phys. Chem. B* **103**, 8612–8617.
26. Dewar, M. J. S., R. C. Bingham and D. H. Lo (1975) Ground-states of molecules. 25. MINDO-3—improved version of MINDO semiempirical SCF-MO method. *J. Am. Chem. Soc.* **97**, 1285–1293.
27. Zerner, M. C. (1991) Semiempirical Molecular Orbital Methods. In *Reviews in Computational Chemistry*, Vol. 2 (Edited by K. B. L. a. D. B. Boyd), pp. 313–365. VCH Publishers, New York.
28. Ridley, J. E. and M. C. Zerner (1976) Triplet-states via intermediate neglect of differential overlap—benzene, pyridine and diazines. *Theor. Chim. Acta* **42**, 223–236.
29. Del Bene, J. and H. H. Jaffe (1968) Use of CNDO method in spectroscopy. I. Benzene pyridine and diazines. *J. Chem. Phys.* **48**, 1807.
30. McEwen, J. and K. Yates (1987) Photohydration of styrenes and phenylacetylenes—general acid catalysis and bronsted relationships. *J. Am. Chem. Soc.* **109**, 5800–5808.
31. Becker, R. S. (1969) *Theory and Interpretation of Fluorescence and Phosphorescence*. Wiley-Interscience, New York.
32. Turro, N. J. (1965) *Molecular Photochemistry*. W. A. Benjamin, New York.
33. Pineiro, M., M. M. Pereira, A. Gonsalves, L. G. Arnaut and S. J. Formosinho (2001) Singlet oxygen quantum yields from halogenated chlorins: potential new photodynamic therapy agents. *J. Photochem. Photobiol. A: Chem.* **138**, 147–157.
34. Braslavsky, S. E. and G. E. Heibel (1992) Time-resolved photothermal and photoacoustic methods applied to photoinduced processes in solution. *Chem. Rev.* **92**, 1381–1410.
35. Scaiano, J. C., R. W. Redmond, B. Mehta and J. T. Arnason (1990) Efficiency of the photoprocesses leading to singlet oxygen (1-Delta-G) generation by alpha-terthienyl—optical-absorption, optoacoustic calorimetry and infrared luminescence studies. *Photochem. Photobiol.* **52**, 655–659.